Journal of Structural Geology 32 (2010) 1317–1333

Contents lists available at ScienceDirect

Journal of Structural Geology

journal homepage: www.elsevier.com/locate/jsg

Oblique normal faulting along the northern edge of the Majella Anticline, central Italy: Inferences on hydrocarbon migration and accumulation☆

Fabrizio Agosta [a,*], Mauro Alessandroni [a,1], Emanuele Tondi [a], Atilla Aydin [b]

[a] Department of Earth Sciences, University of Camerino, Via Gentile III da Varano, 62032 Camerino (MC), Italy
[b] Department of Geological and Environmental Sciences, Stanford University, Stanford, CA 94305-2115, USA

ARTICLE INFO

Article history:
Received 13 December 2007
Received in revised form
11 March 2009
Accepted 19 March 2009
Available online 5 November 2010

Keywords:
Carbonate grainstones
Failure modes
Fault architecture
Fault permeability
Central Apennines

ABSTRACT

Along the northern edge of the Majella anticline, in a large quarry originally excavated by ancient Romans, we studied the deformation mechanisms and internal architectures of faults characterized by both normal and lateral components of slip. These oblique normal faults, which crosscut Miocene carbonate grainstones, are associated with hydrocarbons in the form of tar. Within the faults, tar is present in the breccia of the fault cores, as well as in the surrounding fractured and faulted damage zones. Outside of them, tar is found within the porous carbonate beds flanking the oblique normal faults. We propose a conceptual model of fault nucleation and development. In this model, incipient faulting was characterized by shearing of the pre-existing pressure solution seams and formation of two main sets of tail pressure solution seams. With ongoing faulting, exhumation, and growth of the Majella anticline, the main deformation mechanism switched to predominant opening-mode failure in the form of tail joints and veins within the evolving oblique normal faults. This processes allowed the linkage of isolated slip surfaces across contiguous carbonate beds, and the development of isolated pods of fragmented rocks along the evolving faults. Brecciation and cataclasis localized only along the main slip surfaces of the oblique normal faults, forming a zone of intense deformation, the fault core, surrounded by less-deformed fractured, faulted and fragmented carbonates of the damage zone.

Tar distribution was used as a proxy for fault and fracture permeability. Well-developed oblique normal faults, as a whole, form combined barrier-conduit structures to fluid flow. The cataclastic rocks, if continuous along the fault cores, form seals for cross-fault fluid flow, whereas the fault breccia and the surrounding carbonate damage zones act as conduits to fluid flow. Less-evolved oblique normal faults may form either distributed or localized conduits for fluid flow, depending on the presence (distributed) or absence (isolated) of fragmented carbonates around the conductive slip surfaces. Due to their orientation, these faults enhance the overall fault parallel fluid flow, which is thus prominent in the damage zones of the larger faults. The fundamental structural elements with greater tar content are sub-parallel to the current σ_{hmax} of central Italy, reflecting the possible control exerted by the stress state on the overall fault and fracture permeability. At a larger scale, as suggested by the structural location of the study quarry, hydrocarbons are channeled primarily within the releasing jogs of interacting oblique normal faults.

1. Introduction

Under geological loading conditions, at shallow crustal levels, faulted carbonate rocks show a quite variable mechanical behavior. Carbonate rocks like dolomites deform primarily by an opening-mode-based mechanism, as documented for strike-slip faults that developed from the hierarchical formation, and subsequent shearing, of several sets of joints and veins (Mollema and Antonellini, 1999). Under similar conditions, other types of carbonate rocks such as limestones might be also prone to opening-mode deformation (Mazzoli and Di Bucci, 2003), as well as to dissolution (Alvarez et al., 1978; Marshak et al., 1982). This latter mechanisms was documented along normal faults (Graham et al., 2003) and strike-slip faults (Salvini et al., 1999; Antonellini et al., in press) of Italy, which initiated and evolved by formation, and subsequent shearing, of numerous sets of pressure solution seams. Often, both mechanisms leading to jointing and dissolution occur

DOI of original article: 10.1016/j.jsg.2009.03.012.
☆ A publishers' error resulted in this article appearing in the wrong issue. The article is reprinted here for the reader's convenience and for the continuity of the special issue. For citation purposes, please use the original publication details; Journal of Structural Geology, 31(7), pp. 674–690.
* Corresponding author.
E-mail address: fabrizio.agosta@unicam.it (F. Agosta).
[1] Present address: BEICIP-FRANLAB, Rueil-Malmaison, France.

0191-8141/$ – see front matter © 2009 Elsevier Ltd. All rights reserved.
doi:10.1016/j.jsg.2010.10.007

during faulting of platform, slope and basinal carbonate rocks (Rispoli, 1981; Petit and Mattauer, 1995; Willemse et al., 1997; Kelly et al., 1998; Kim et al., 2003; Agosta and Aydin, 2006; Antonellini et al., in press). Additionally, porous rocks like carbonate grainstones can behave as a granular material when loaded (Aydin et al., 2006), deforming primarily by compaction and shear banding (Tondi et al., 2006; Tondi, 2007).

Fault-related fundamental structural elements such as joints, pressure solution seams, sheared joints and pressure solutions, compaction and shear bands may have different effects on subsurface fluid flow (Aydin, 2000). Joints, as opening-mode fractures (Pollard and Aydin, 1988), form conduits for fluid flow. On the contrary, pressure solution seams, as closing-mode fractures (Fletcher and Pollard, 1981), often contain films of residual, undissolved, impermeable clay-rich material. Nevertheless, when sheared, pressure solution seams may channel fluids within the thin volume of fragmented carbonates they include (Graham-Wall et al., 2006). Compaction bands are thought to always inhibit the fluid flow because of their lower value of porosity with respect to the surrounding porous host rock (Tondi et al., 2006). Conversely, shear bands can act either as barriers or conduits to fluid flow, depending on their mechanical processes (Aydin et al., 2006).

The aforementioned fundamental structural elements are generally displayed along incipient faults, as well as in the least-deformed portions of the fault damage zones which consist of fractured, fragmented and faulted rocks that did not obliterate the original host rock features (Cowie and Scholz, 1992; Kim et al., 2004; Odling et al., 2004; Flodin and Aydin, 2004; Agosta and Aydin, 2006). Damage zones generally flank the fault cores, which are rock volumes with higher values of deformation intensity. Brecciation, comminution, dissolution/precipitation, and other mechanical, chemical, and diagenetical processes generally take place in the fault cores, destroying therefore the original host rock fabric (Sibson, 1977; Chester and Logan, 1986; Blenkinsop, 1991; Chester et al., 1993; Antonellini and Aydin, 1994; Billi, 2005; Mort and Woodcock, 2008). Both core and damage zones are sandwiched by pristine host rocks characterized by background values of deformation intensity. Based on the relative thickness, petrophysical properties, lateral continuity, and overall architecture of core and damage zones, faults can act either as conduits or barriers

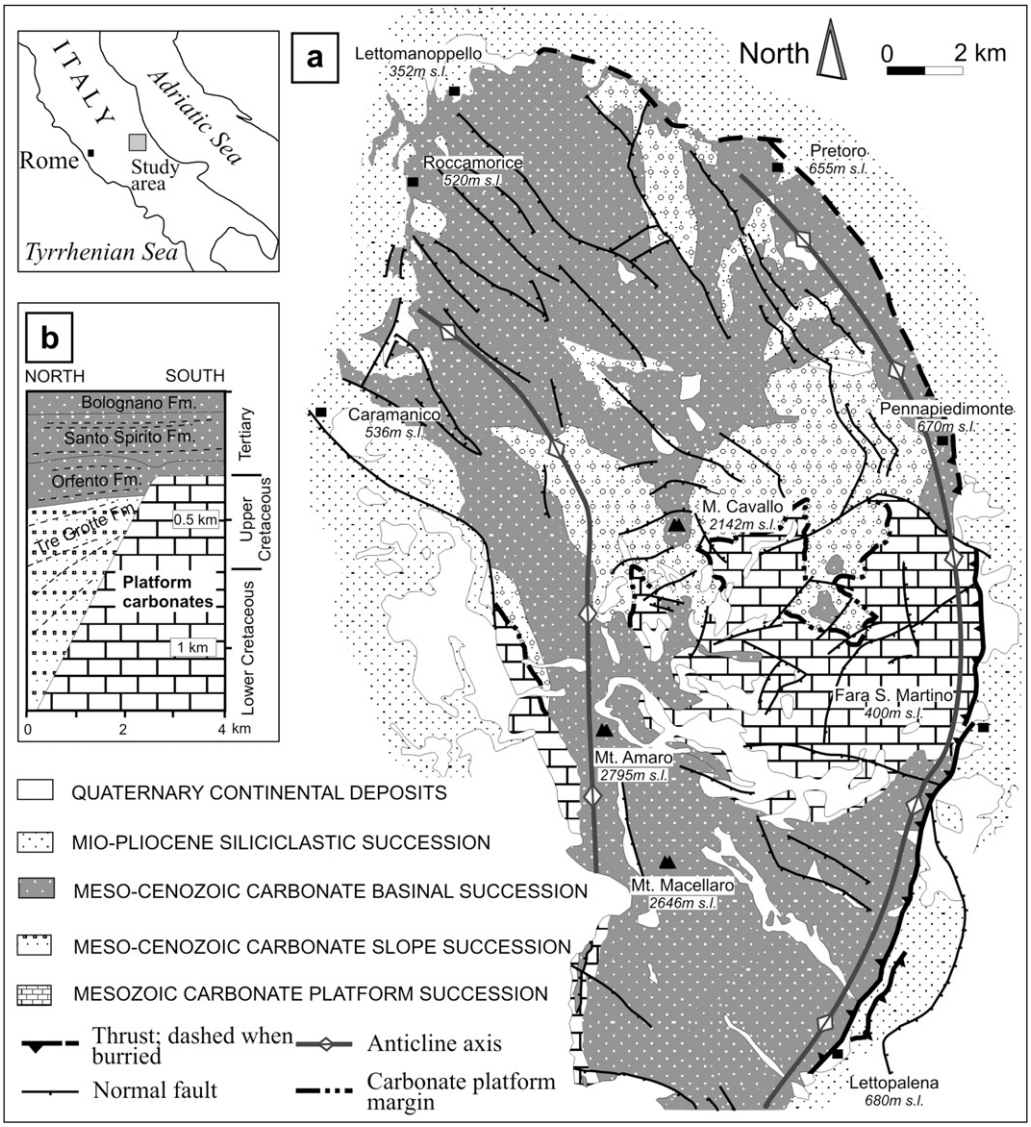

Fig. 1. (a) Geological map of the Majella Mountain (modified after Vezzani and Ghisetti, 1998); the rectangle represents the location of Fig. 2(a). (b) Simplified stratigraphic section of the carbonate platform margin.

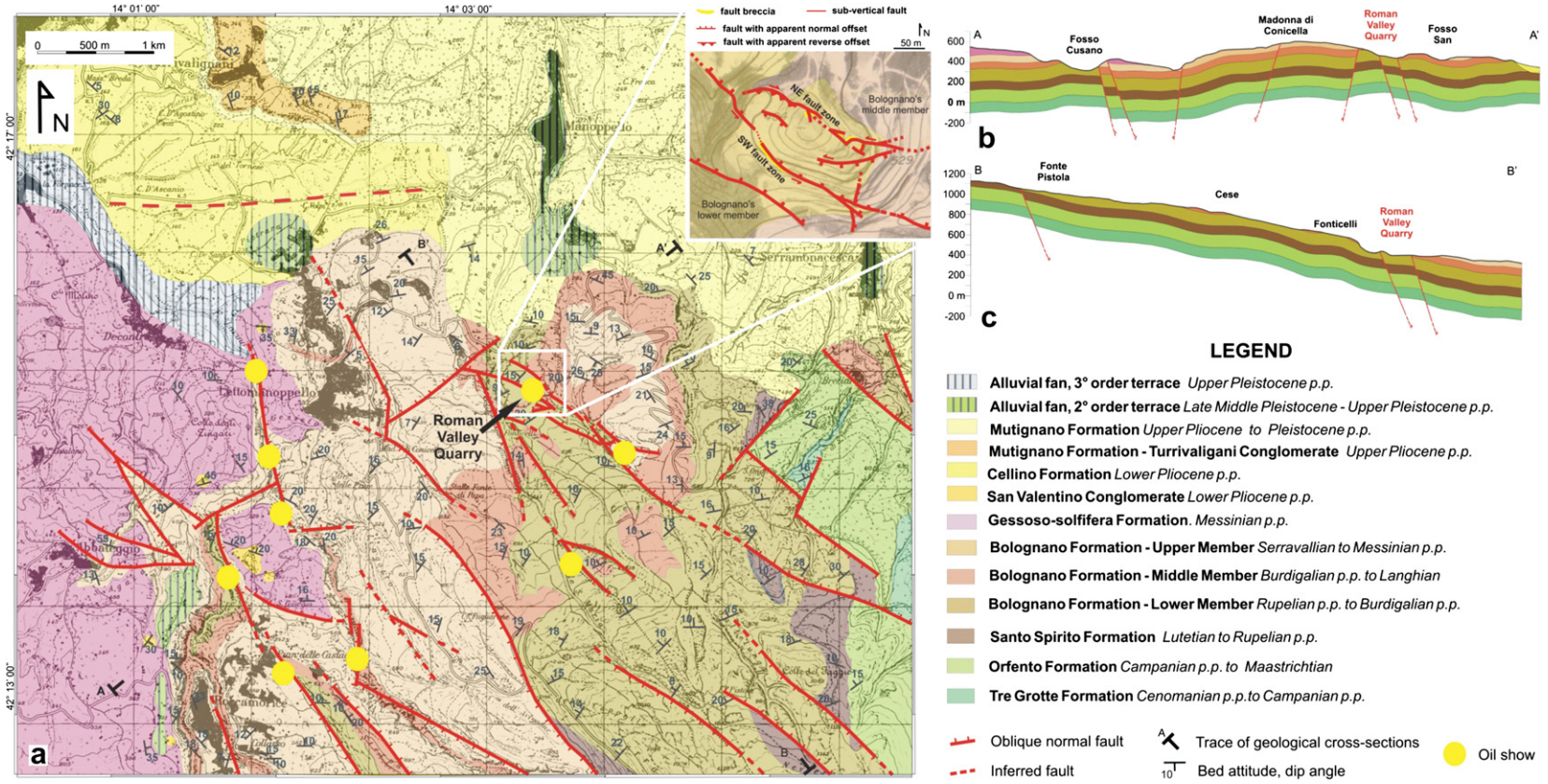

Fig. 2. (a) Geological map of the northern portion of the Majella Mountain showing formations, major faults, and oil shows. The inset shows the structural arrangement of the Roman Valley Quarry area. (b) and (c) Geological cross-sections of the study area.

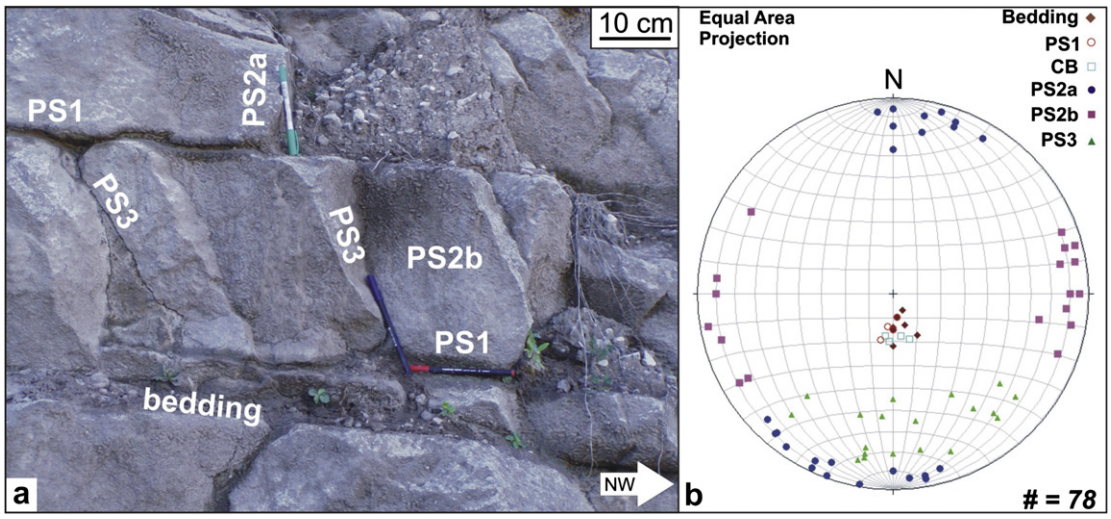

Fig. 3. (a) Outcrop view of unfaulted carbonate grainstones pertaining to the lower member of the Bolognano Formation. In this figure, the main structures related to both burial-related and folding and thrusting structural assemblages are reported. (b) Lower hemisphere equal area projection of the poles representing the fundamental structures.

to fluid flow, or may form combined barrier-conduit permeability structures (Antonellini and Aydin, 1994; Caine et al., 1996; Ghisetti et al., 2001; Rawling et al., 2001; Agosta and Kirschner, 2003; Storti et al., 2003; Billi et al., 2003; Flodin et al., 2005; Micarelli et al., 2006; Agosta et al., 2007).

In order to better understand the mechanisms of fault initiation and development in carbonate rocks, and their control on fault architecture and permeability, we study high-angle oblique normal faults crosscutting carbonate grainstones of the Majella Mountain, central Italy. The Majella stratigraphy consists of a marine carbonate sequence that includes platform, slope, and basinal deposits of Meso-Cenozoic age (Vezzani and Ghisetti, 1998). Due to the variety of carbonate rocks and depositional sequences, the Majella Mountain provides a great opportunity to study how deformation is controlled by this heterogeneous depositional system (Graham et al., 2003; Marchegiani et al. 2006; Tondi et al., 2006; Antonellini et al., in press; Aydin et al., this issue), representing a good analogue for fractured reservoirs (Lampert et al., 1997). Furthermore, presence of hydrocarbons in the form of tar residue in several portions of the Majella Mt. offers an extraordinary occasion to study the control exerted by fractures and faults on subsurface fluid migration and accumulation.

2. Geological setting

The Majella is a thrust-related, box-shaped anticline. It is comprised of the Majella Mountain unit overlying the Casoli unit. These units crop out in the outer part of the central Apennine fold-and-thrust belt, override the eastern Adriatic foreland and are, in turn, overridden by the Morrone Mt. unit, to the west, and by the Molise and Sicilide units, to the east (Vezzani and Ghisetti, 1998). The Majella Mountain unit is comprised of a carbonate sequence of Lower Cretaceous to Miocene age, which is topped by siliciclastic sediments of Messinian-Lower Pleistocene age (Fig. 1(a)). The Cretaceous sequence consists of platform limestones originally pertaining to the Apulian realm, in the south and in the center of the mountain, and slope-basinal carbonates, in the north (Eberli et al., 1993; Vecsei et al., 1998). The Cenozoic sequence is comprised of a carbonate ramp sequence on top of the Cretaceous carbonate platform and its margins, in the center; conversely, further to the north this sequence consists primarily of basinal carbonate rocks (Fig. 1(b)).

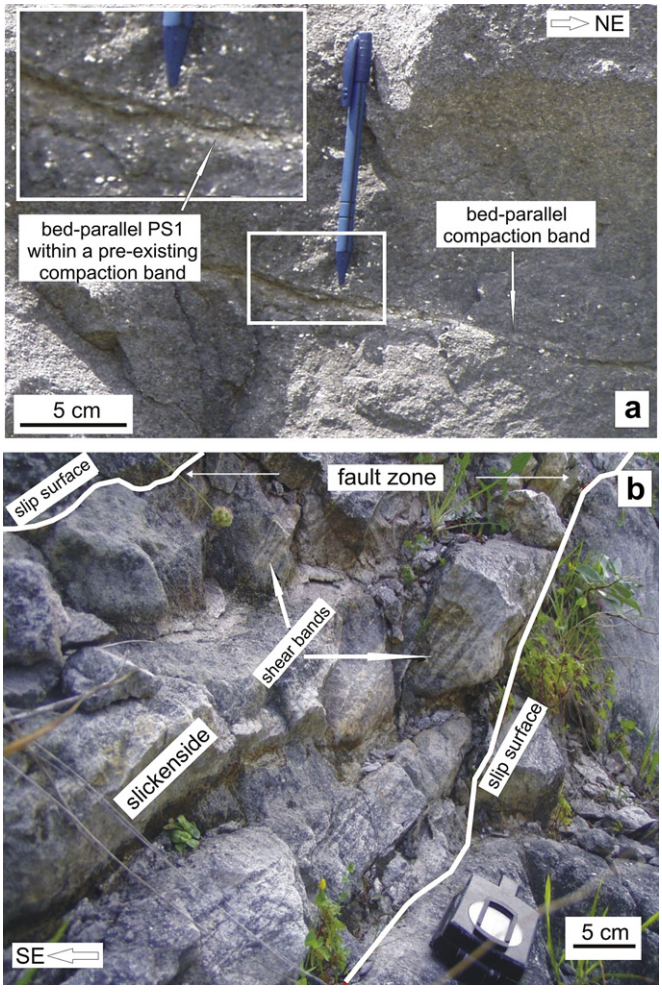

Fig. 4. (a) Picture of a bed-parallel compaction band that formed in the most porous carbonate beds (ϕ up to 30%) pertaining to the lower member of the Bolognano Formation. The inset shows a close-up of this compaction band. (b) Plan view of a shear bands zone bounded by two main slip surfaces. In the field, the individual bands are easily recognizable by their light colour relative to the surrounding, tar-invaded porous carbonate grainstones.

The Majella anticline is characterized by a steeply dipping, to overturned, eastern flank and a more gently-dipping western flank (Fig. 1(a)). Both fold axes of this non-cylindrical fold, which are subparallel to each other, plunge both north and south. Folding and thrusting of the Majella Mt. occurred during the Middle–Upper Pliocene, as recorded by the angular unconformity between Lower Pliocene and Upper Pliocene–Lower Pleistocene siliciclastic sediments (Vezzani and Ghisetti, 1998), during a regional episode of shortening that involved the whole Apenninic foredeep (Bally et al., 1988). Shortening was followed by uplift, as in the rest of central Apennines (Ghisetti and Vezzani, 1999), with rates that vary between 1.4 and 2.5 mm/yr considering rocks of 3.5 and 1.6 Ma, respectively.

The western limb of the anticline is truncated by the Caramanico normal fault, which is characterized by a maximum throw of ~4 km and pronounced along-strike variations of the offset (Ghisetti and Vezzani, 2002). By considering the crosscutting relations among the Caramanico normal fault, the fold axes, and the western limb of the anticline, these authors proposed that, at least a major episode of, normal faulting postdated the Majella's folding and thrusting. Conversely, other authors considered the Caramanico fault as a pre-existing, hinterland-dipping normal fault of Messinian age (Scisciani et al., 2002). Along with this model, the latter authors inferred an Early Pliocene age for the large normal fault bounding the eastern forelimb of the Majella anticline. At a larger scale, taking into account the whole Majella Mountain, Marchegiani et al. (2006) recognized that folding and thrusting were associated with normal and strike-slip faulting.

2.1. Study area

The study area is located along the northern termination of the Majella Mountain, around the village of Lettomanoppello (Fig. 2(a)). There, the carbonate beds dip generally 10°–25° to NE, so that the whole basinal sequence youngs downslope. The northern boundary of

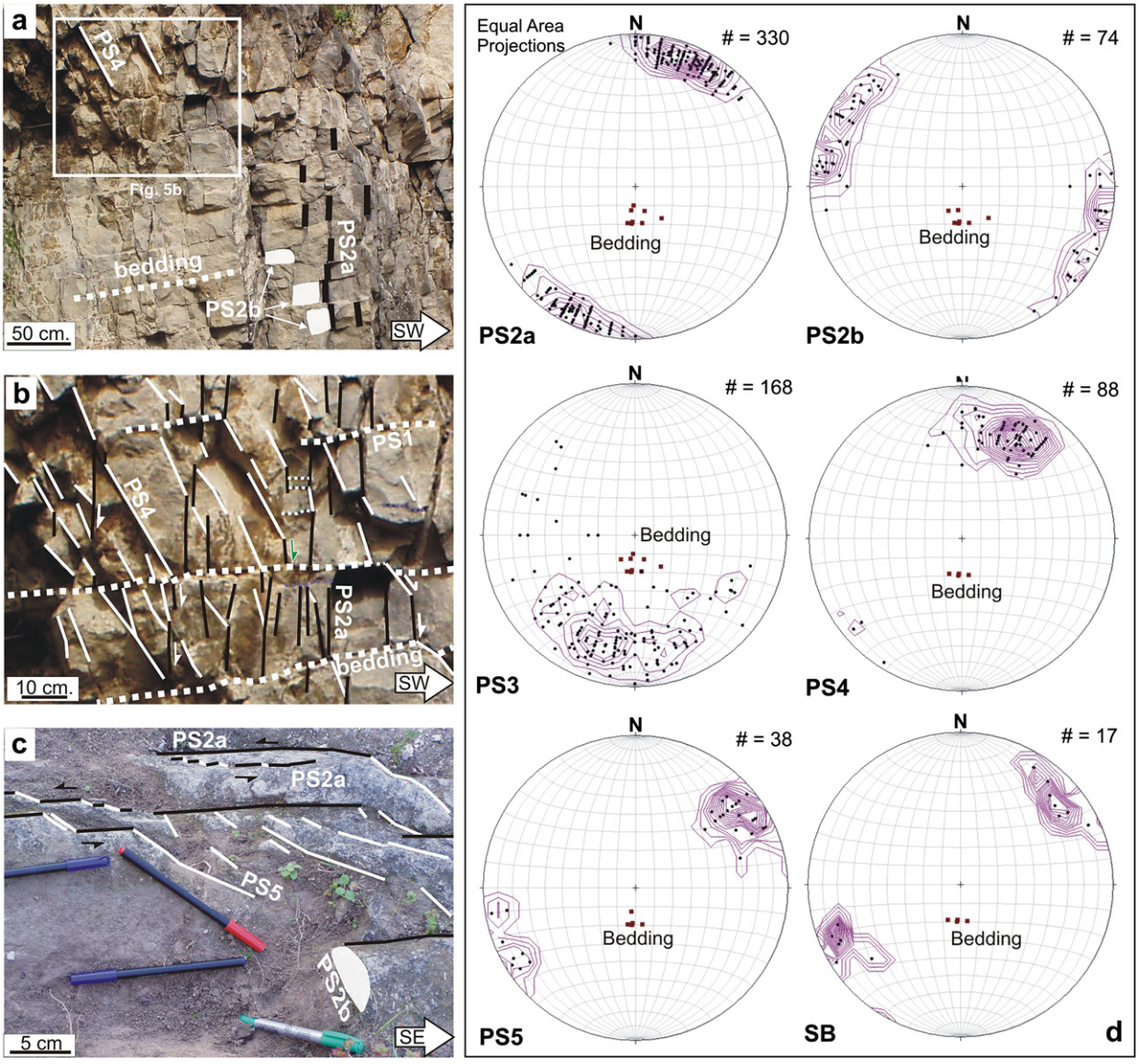

Fig. 5. (a) Cross-sectional view of incipient normal faults. Tail PS4 located at the contractional quadrants of normal sheared, pre-existing PS2a elements. The dashed rectangle represents the location of Fig. 5(b). (b) Close-up of the abutting relationships among the different PS elements. Tail PS4 terminates against the normal sheared PS2 elements; both of them are confined within the individual carbonate beds. (c) Plan view of incipient strike-slip faults. Tail PS5 displayed at the contractional quadrants of left-lateral sheared PS2a elements. (d) Lower hemisphere equal area projection of the poles, and relative density contour plot, representing the main structural elements.

this area is marked by Lower Pliocene clays and marls, ascribed to either Cellino Formation (Casnedi, 1983) or Majella flysch (Patacca et al., 1992), and by Upper Pliocene–Lower Pleistocene siltstones and clays of the Mutignano Formation (Ghisetti and Vezzani, 1998). The western boundary is defined by shales, marls, limestones, and gypsum of Messinian age (Gessoso-Solfifera Formation, Selli, 1960), whereas both eastern and southern edges are marked by Upper Cretaceous porous carbonate grainstones of the Orfento Formation (Vecsei, 1991) and Paleocene to Upper Oligocene pelagic, shallow-water limestones of the Santo Spirito Formation (Crescenti et al., 1969).

As shown in Fig. 2(a), faults in this area strike primarily NW, dipping either NE or SW. The individual faults are up to a few km-long, and are characterized by apparent normal offsets on the order of several tens of meters (Fig. 2(b) and (c)). Secondary faults, which strike NE and dip NW, abut against the first set. These NE-oriented faults are up to about 1 km-long, and also have apparent normal offsets. Although the Upper Pliocene–Lower Pleistocene sediments show vague evidences of internal deformation (cf. Fig. 2(a)), the faulting activity occurred in the study area until the Middle Pleistocene, which is the age of the slope deposits covering the faults.

Our detailed structural analyses were carried out along the vertical outcrops and the few pavements of the Roman Valley Quarry, which display in 3D the internal structures of high-angle faults (cf. inset of Fig. 2(a)) crosscutting the lower member of the Bolognano Formation (Donzelli, 1997). This member, up to 100 m-thick, is made up of medium-to-coarse grained carbonate grainstones with calcirudite and marl-rich intercalations. Within the quarry, we mapped its walls and pavements by using ground photo mosaics as base-maps, by taping acetate sheets to the outcrops, and by performing string-line mapping.

3. Structural analysis

Performing the structural analyses of the different elements associated to pre-faulting deformation and of those related to faulting, we mainly considered their geometry, orientation, internal structure, infilling material (if present), possible offset, and the crosscutting and abutting relationships with respect to the surrounding other elements. Fractures were distinguished as mode I (joints), anti-mode I (pressure solution seams), sheared joints and sheared pressure solution seams. Deformation bands were classified based on their orientation with respect to bedding, as well as on the possible offset resolved across these elements. Most of the faults cropping out in the quarry are characterized by apparent

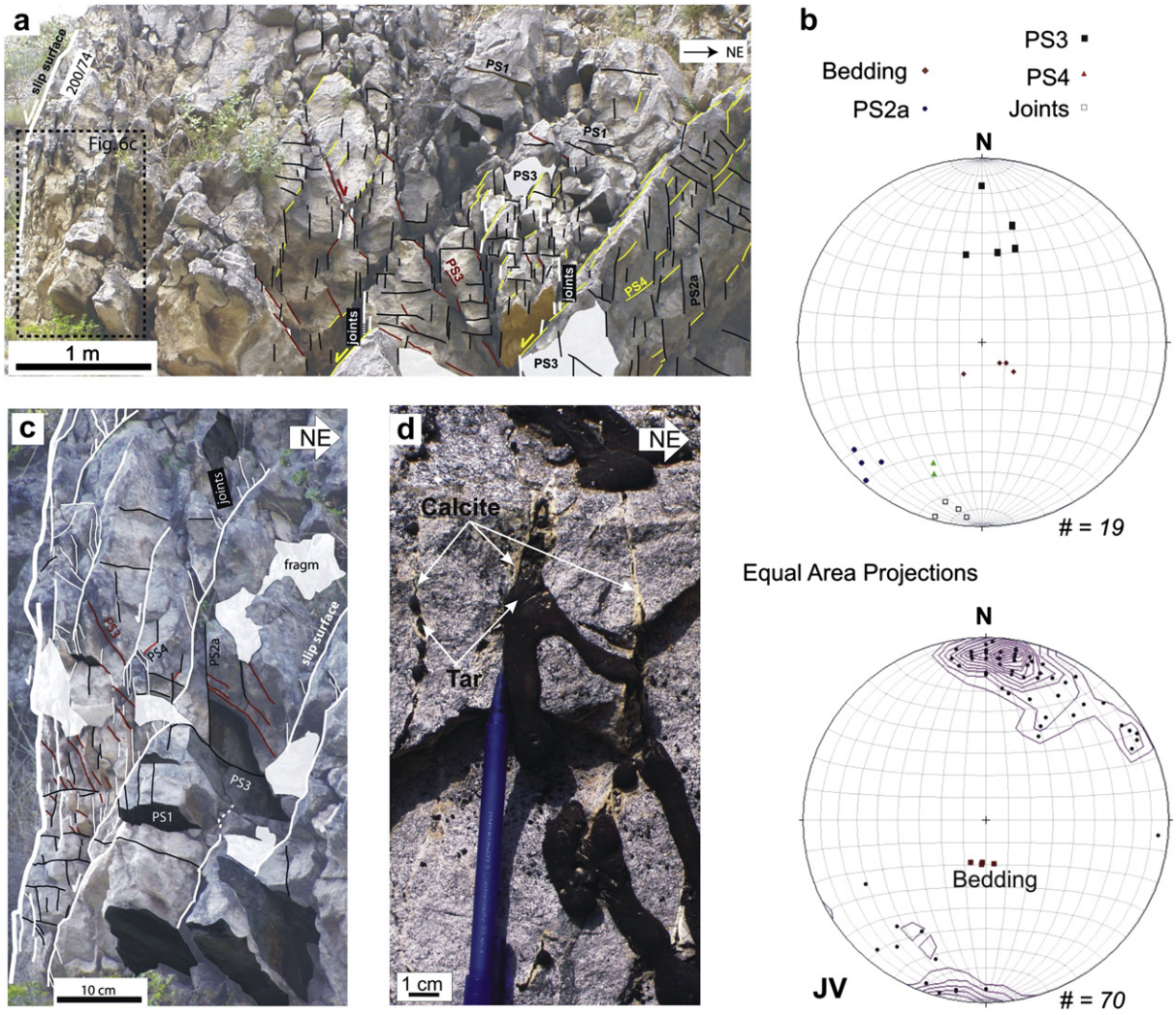

Fig. 6. (a) Structural elements present along small normal faults. The dashed rectangle represents the location of Fig. 6(c). (b) Lower hemisphere equal area projection of the poles relative to some of the structural elements of Fig. 6(a), above, and of all JV elements measured in the quarry. (c) Close-up of small normal faults made up of through-going slip surfaces and tail joints/veins, which localized at their extensional quadrants and/or at the releasing jogs. (d) Calcite- and tar-filled veins, located at the extensional quadrant of a through-going slip surface (not shown in the figure).

normal offsets; only in a few cases we were able to document apparent reverse offsets. Based on their total lengths and offsets, we classify the faults into four different classes: incipient (length < 1 m, offset < a few cm), small (1 m < length < 10s m, a few cm < offset < 10 cm), medium (10's m < length < 100 m, 10s cm < offset < about 1 m), and large faults (length > 100's m, offset > a few m).

3.1. Background deformation

The study area exposes the upper part of the Bolognano Formation's lower member, which is mainly comprised of carbonate grainstones, as well as a small portion of marls and calcareous marls (middle member). Far from the faults, four main sets of pressure solution seams (PS) and one set of deformation bands crosscut the unfaulted carbonate grainstones. The PS consist of one set of bed-parallel (PS1), two sets of orthogonal bed-perpendicular (PS2a and PS2b, respectively), and one set of pressure solution seams oblique to bedding (PS3). All four PS are portrayed in Fig. 3(a), and their orientations are plotted in Fig. 3(b).

The bed-parallel PS1 have a columnar form and localize in the carbonate beds, at the contacts between adjacent beds, as well as within early-formed bed-parallel deformation bands. Most PS1 show evidences of shearing. The two orthogonal bed-perpendicular sets are present within the carbonate beds, crosscut each other, and are often bounded by PS1. Both PS2a and PS2b have generally a wavy form, contain mm-thick clay-rich residue material and, in some cases, show evidences of shearing. PS2a strike E–W to NW–SE and dip more than 70° either N or S; PS2b strike about N–S and dip more than 75° either E or W. PS3 have a wavy irregular form, contain mm-thick clay-rich residue material, and abut against PS1, PS2a and PS2b. Attitudes of PS3 are quite variable; most of them strike E–W and dip 45°–70° N. Individual PS3 localize at the contractional tips and/or irregularities of the sheared PS1.

In most porous carbonate grainstone beds, which have porosity (ϕ) values up to ~30% relative to the 5–20% range of most carbonate beds (data obtained after thin-sections digital image analysis, Rustichelli, personal communication), there are bed-parallel deformation bands. At an outcrop scale, these elements are lighter than the parent rocks (Fig. 4(a)), are up to a several tens of cm-long and 0.5–3 mm-thick. At a thin-section scale, they have lower values of porosity and similar grains/matrix values relative to the parent rocks. No evidence of shearing across these bands has been found in the field or under the microscope. All these observations are consistent with these bed-parallel elements being compaction bands (CB), similar to those documented by Tondi et al. (2006) and Antonellini et al. (in press) in nearby outcrops of the Orfento Fm.

3.2. Incipient faults

Along incipient faults, characterized by offsets on the order of ~1 cm, the nature of both sheared parent elements and newly formed ones is well displayed. In the study quarry, we distinguish two main fault-related structures, deformation bands and pressure solution seams. As suggested by the bedding offset, two sets of oblique to bedding shear bands (SB) characterized by apparent normal offsets are present in the most porous carbonate beds (φ up to 30%). SB can occur as single bands, as well as zones of several individual bands (Fig. 4(b)). Single shear bands are several cm-long, up to 2 mm-thick, and often include pressure solution seams and/or discrete, sheared planar discontinuities. In the field, they show a positive relief with respect to the surrounding host rock. SB zones are several m-long, 5–10 cm-thick, and have straight and narrow shapes. These elements are mainly oriented parallel to the surveyed outcrops (cf. Fig. 4(b)), so that the throw was difficult to measure.

In addition to the four sets described above, we distinguish two more sets of pressure solution seams (PS4 and PS5, respectively). PS4 are oriented at a low angle to bedding, whereas PS5 are at a

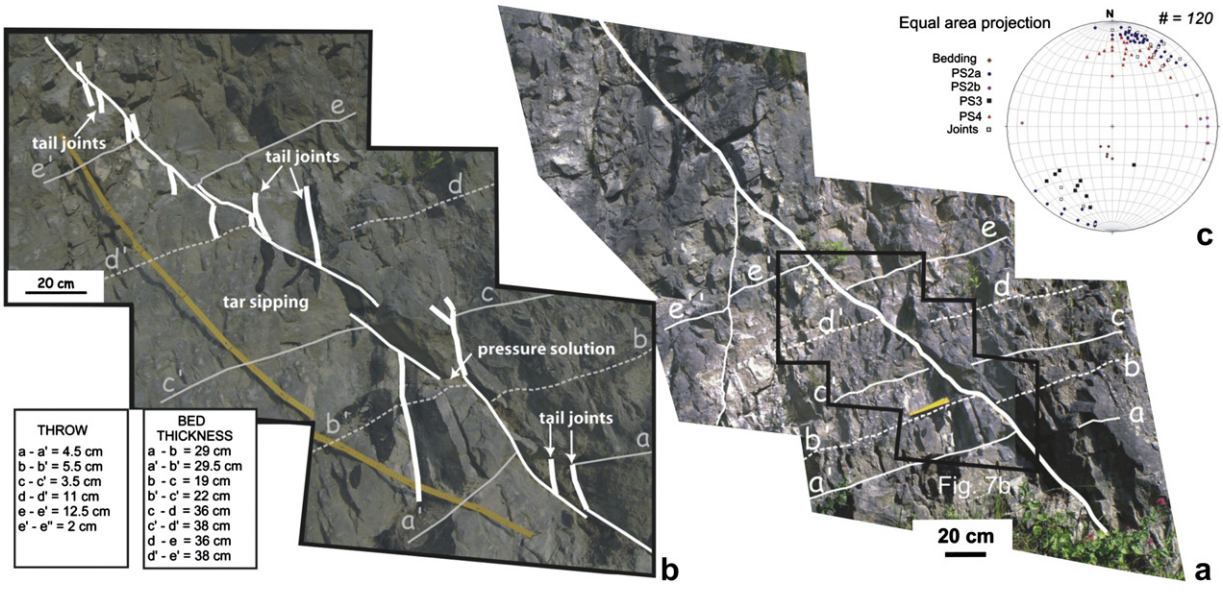

Fig. 7. (a) Normal fault with a throw up to 12.5 cm. In order to calculate the amount of offset, we distinguished five different beds, here named a–e, respectively. The dotted line represents the location of Fig. 7(b). (b) Close-up of the fault. Several isolated slip surfaces are present along the fault, around which tail joints are present at their extensional quadrants and in correspondence of the releasing jogs. Conversely, tail pressure solution seams are present within contractional jogs. The bedding thickness on the two sides of the fault is reported in the lower table, which also shows the amount of vertical offset measured along the individual slip surfaces. (c) Lower hemisphere equal area projection of the poles relative to the different structural elements measured along this fault.

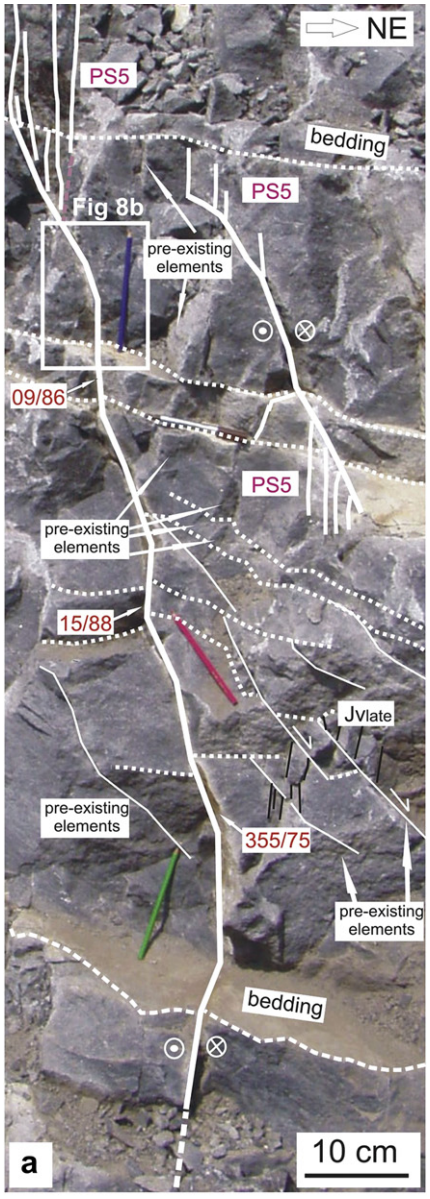

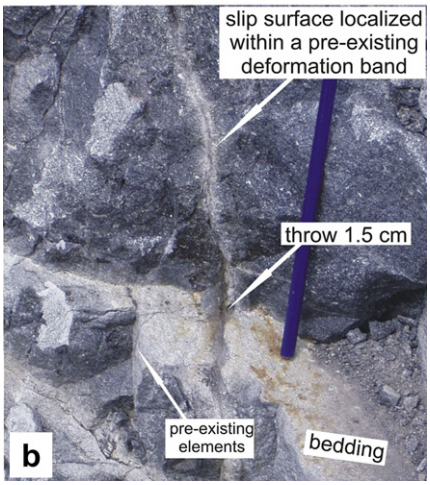

high-angle. Both structures abut against all those pertaining to the background deformation. PS4 have a wavy form, contain mm-thick clay-rich residue material, are up to several cm-long and a few mm-thick. These structures localize in the contractional quadrants of normally sheared PS2a and PS2b seams (Fig. 5(a) and (b)). Some PS4 show evidences of normal shearing. PS5 have a wavy form, include mm-thick clay-rich residual material, and localize in the contractional quadrants and/or irregularities of left-lateral sheared PS2a, as shown in some narrow pavements of the quarry (Fig. 5(c)). PS5 are up to several cm-long, and about 1–2 mm-thick. Along the few outcrops displaying both PS4 and PS5, the latter abut against PS4.

3.3. Small faults

Small normal faults with, at least, a few cm offset are comprised of isolated, discontinuous slip surfaces dipping about 40°–50° both to SW and NE, and cm-long tail joints and veins (JV) at their extensional quadrants (Fig. 6(a)). The discontinuous slip surfaces are oriented sub-parallel to either PS3 or PS4, suggesting that the faults formed on individual PS3 or PS4. JV consist of joints, which do not have any infilling material, and veins containing calcite and/or hydrocarbons in the form of tar. All joints and veins are sub-vertical (Fig. 6(b)), have a length between ~1 cm and several cm, and an opening between a fraction of a mm and a few mm. Joints rarely show their typical features such as rib marks or hackles (Pollard and Aydin, 1988), making their identification in the field quite difficult to accomplish.

The relationship between tail JV and slip surfaces is more evident along more evolved faults, in which the slip surfaces cut across several carbonate beds (Fig. 6(c)). There, the tail joints localize within releasing jogs formed by interacting slip surfaces. The joints determine their coalescence across contiguous carbonate beds, and formation of isolated pods of fragmented rocks. Veins, when present, generally contain calcite and tar (Fig. 6(d)).

In some case, both tail JV and PS are present at the extensional and contractional quadrants, respectively, of individual slip surfaces. The internal structure of a small normal fault with a throw of up to 12.5 cm is made up of several, short, discontinuous slip surfaces and both tail joints and tail pressure solution seams (Fig. 7 (a–c)). Tail JV and PS are also present along small faults with predominantly left-lateral slip, which have offsets on the order of a few to several cm (Fig. 8(a)). There, a through-going slip surface localized within pre-existing structural elements, such as the shear bands shown in Fig. 8(b), cutting across several carbonate beds.

3.4. Medium faults

Faults with offsets on the order of several 10s of cm include an inner core, which is made up of discontinuous brecciated and fragmented carbonate pods around a through-going main slip surface, and less-deformed carbonates of the damage zone. Considering a normal fault with a maximum throw of 36 cm, the carbonate rocks of the damage zone are crosscut by at least two generations of tail opening-mode fractures (Fig. 9(a)). Their abutting relations are consistent with formation of a first generation of tail veins at the extensional quadrants of the evolving main slip surface, their subsequent shearing, and the consequent localization of a second generation of tail joints at their extensional quadrants.

Fig. 8. (a) Left-lateral fault with a throw of about 1.5 cm. As suggested by the attitude variations of the main slip plane, here reported by dip azimuth and dip angle, this fault formed due to the linkage of pre-existing PS2a, PS3, and shear band elements. The dashed rectangle represents the location of Fig. 8(b). (b) Close-up of the main fault plane crosscutting two different carbonate beds. The through-going slip surface localizes within a pre-existing shear band, as suggested by its lighter colour with respect to the parent rock.

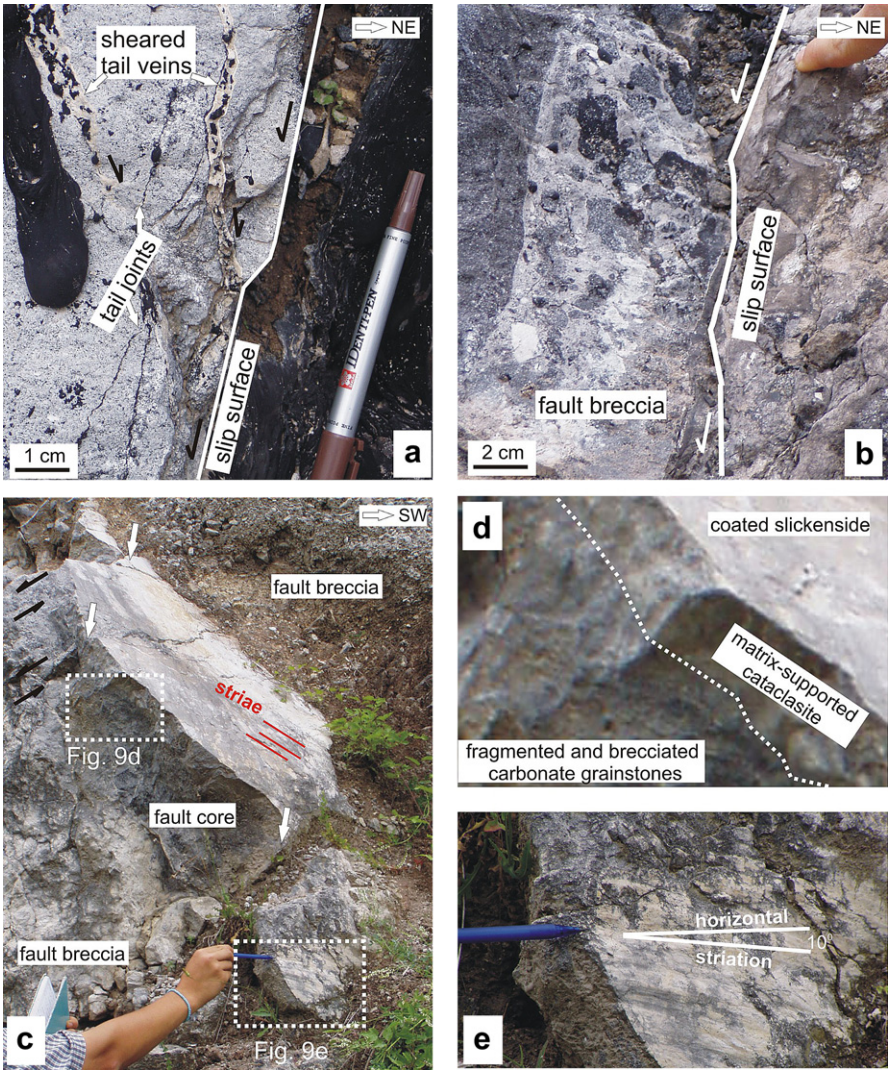

Fig. 9. (a) Close-up of calcite- and tar-filled veins present at the extensional quadrant of a through-going slip surface. These veins were subsequently sheared generating a second generation of tail opening-mode fractures. (c) Close-up of a coarse grained fault breccia bounded by a through-going slip surface. Some of the clasts included show tar impregnation. (c) Close-up of the main slip surface of a fault with a throw of about 2 m. The major slip surface is coated by calcite cements and crosscut by sheared, orthogonal fractures (indicated by yellow arrows). Striation along this surface is consistent with normal-sinistral offset. The white dotted rectangles represent the location of Fig. 9(d) and (e). (d) Close-up of matrix-supported cataclasites that surround the major slip surface. (e) Close-up of the oblique striations present along a slip surface of the fault core. (For interpretation of the references to colour in this figure legend, the reader is referred to the web version of this article).

The pods of fault breccias cropping out along the same fault are comprised of angular carbonate fragments embedded in a finer matrix (Fig. 9(b)).

Faults with offsets on the order of a few meters display more developed fault cores, which may include brecciated and fragmented and major slip surfaces as well as cataclastic rocks, surrounded by fractured and faulted carbonate damage zones. Along a fault with a maximum throw of about 2 m (Fig. 9(c)), the fault core of matrix-supported cataclasites (Fig. 9(d)) and coated slip surfaces with oblique striations (Fig. 9(e)) is crosscut by opening-mode fractures subsequently sheared with a normal sense of slip (yellow arrows on Fig. 9(c)).

3.5. Large faults

The two large faults of the Roman Valley Quarry, labeled SW and NE (Fig. 10(a)), have vertical throws of about 40 m and 10 m, respectively. Both faults down drop their eastern side. The SW fault is comprised of two main segments oriented ~N290E to ~N300E, dipping about 75° N, which form a contractional jog in the northern part of the quarry (cf. inset on Fig. 2(a)). On the contrary, the NE fault is made up of several smaller segments oriented ~N270 to ~N315, dipping 60°–80° either S or N, which form several contractional and releasing jogs. Based on striations of the major slip surfaces, bedding offsets, internal architecture, as well as on the kinematics of smaller faults present within their damage zones, both faults have overall oblique normal components of slip.

The SW fault is made up of a fault core wide up to 1 m, flanked by wide damage zones (Fig. 10(b)). The fault core includes major slip surfaces, fault breccias and cataclastic rocks. Striations along the major slip surfaces are consistent with normal and left-lateral components of slip. The fault breccia, which makes most of the fault core, is generally bounded by major slip surfaces (Fig. 10(c)). Cataclasites are up to a few cm-thick, and consist of survivor carbonate clasts, sub-angular to rounded in shape, surrounded by (grain-supported) or embedded in (matrix-supported) a carbonate matrix. Under the microscope, the cataclasites show presence of secondary calcite cements, which also coat the major slip surfaces (Fig. 10(d)). The damage zone of this fault is made up of several generations of tail fractures, small faults, and intermediate faults. Based on the

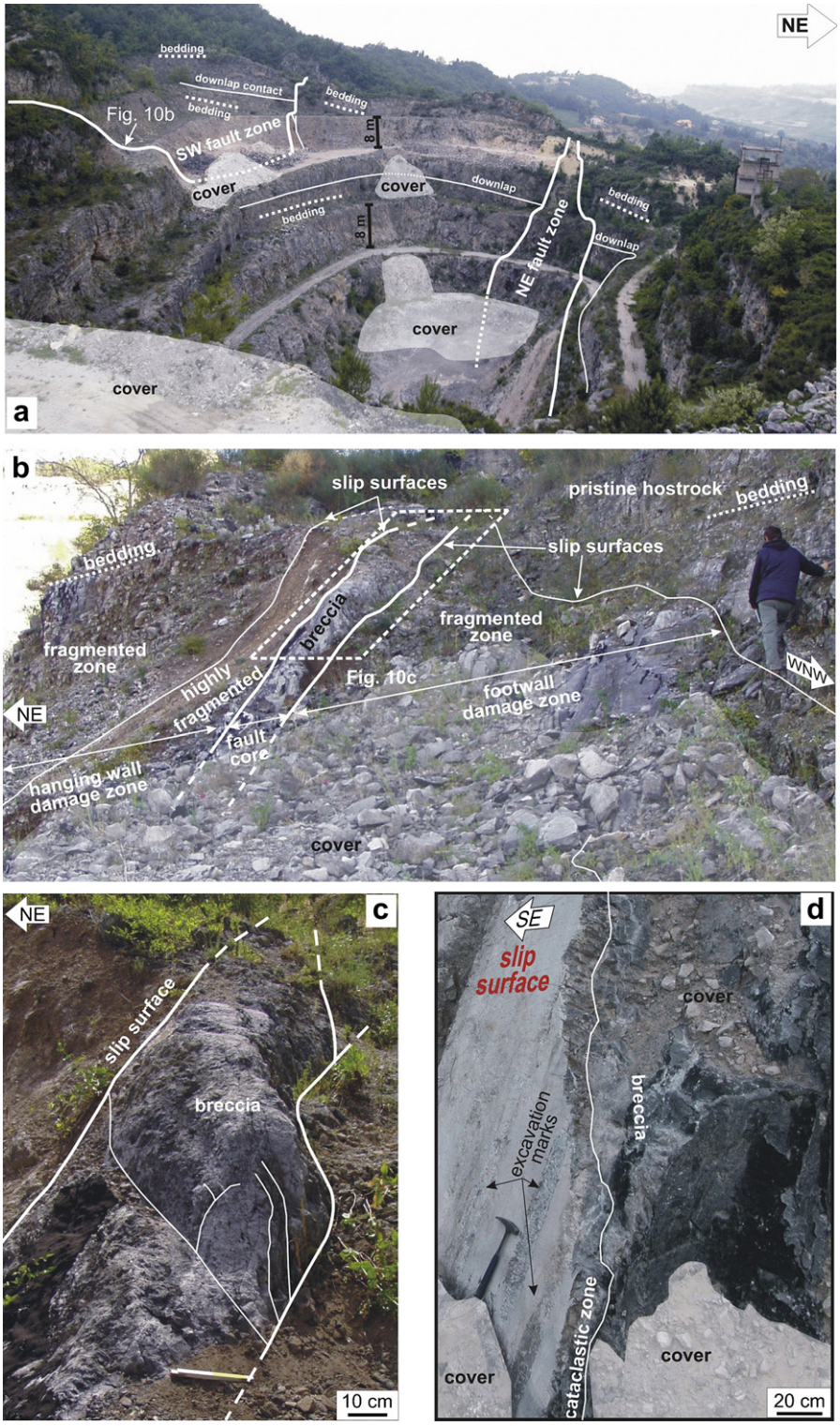

Fig. 10. (a) Northern and western walls of Roman Valley Quarry view due to south. Two main faults, here respectively named SW and NE, are reported. The amount of throw across each fault has been estimated by the offset of a sedimentary downlap contact of the lower Bolognano member. (b) Internal architecture of the SW fault. A meter-thick highly fragmented zone is present at the boundary with the fault core in the hanging wall damage zone. The dotted rectangle represents the location of Fig. 10(c). (c) Close-up of the fault breccia, which is bounded by major slip surfaces. (d) Cross-sectional view of the main fault plane, which is flanked on the footwall side by a cm-thick cataclastic zone.

quarry's outcrops, the hanging wall damage zone is about twice as wide as that of the footwall.

Along the northern portion of the quarry, the NE fault is comprised of one main fault segment oriented N270E, which displays an apparent reverse offset (cf. inset in Fig. 2(a)). Both orientation and striations of the main slip surfaces suggest a pronounced right-lateral component of slip along this fault, whereas elsewhere it is characterized by normal and/or left-lateral components of slip. The overall internal structure of this fault is comprised of a 6 m-wide fault core, which includes

discontinuous pods of fault breccias, intensively deformed carbonate rocks and major slip surfaces, surrounded by less-deformed carbonate rocks (Fig. 11(a) and (b)). Along this fault, the intersections among three or more main slip surfaces are marked by a few m-thick, triangular-shaped fault breccias (Fig. 11(a)). Conversely, jogs formed by two contiguous, sub-parallel slip surfaces are characterized by elongate, 10s of cm-thick, lithon-shaped fault breccias (Fig. 11(b)).

Along the NE fault, at the footwall of one of the main breccias-bounding slip surfaces, there are tightly-spaced, bed-bounded, closed fractures forming sub-parallel clusters, as wide as 50 cm, at a high-angle with respect to bedding. The individual structures, oriented N85 to 130E and dipping either N or S of 60–85°, are PS sub-parallel to sheared PS2a of the carbonates nearby. The kinematics of these structures, which are likely to be sheared, are not clear because they have minimal amount of shearing (Fig. 11(c)). Overall, depending on their orientation, striations of the main slip surfaces mapped along the NE fault show both normal and oblique components of slip (Fig. 11(d–f)). The two main sets of slip surfaces strike NE and E, respectively, and mainly dip S ~60°–75°. Surfaces oriented E–W mainly display normal movements, whereas those oriented NE show normal-sinistral components of slip.

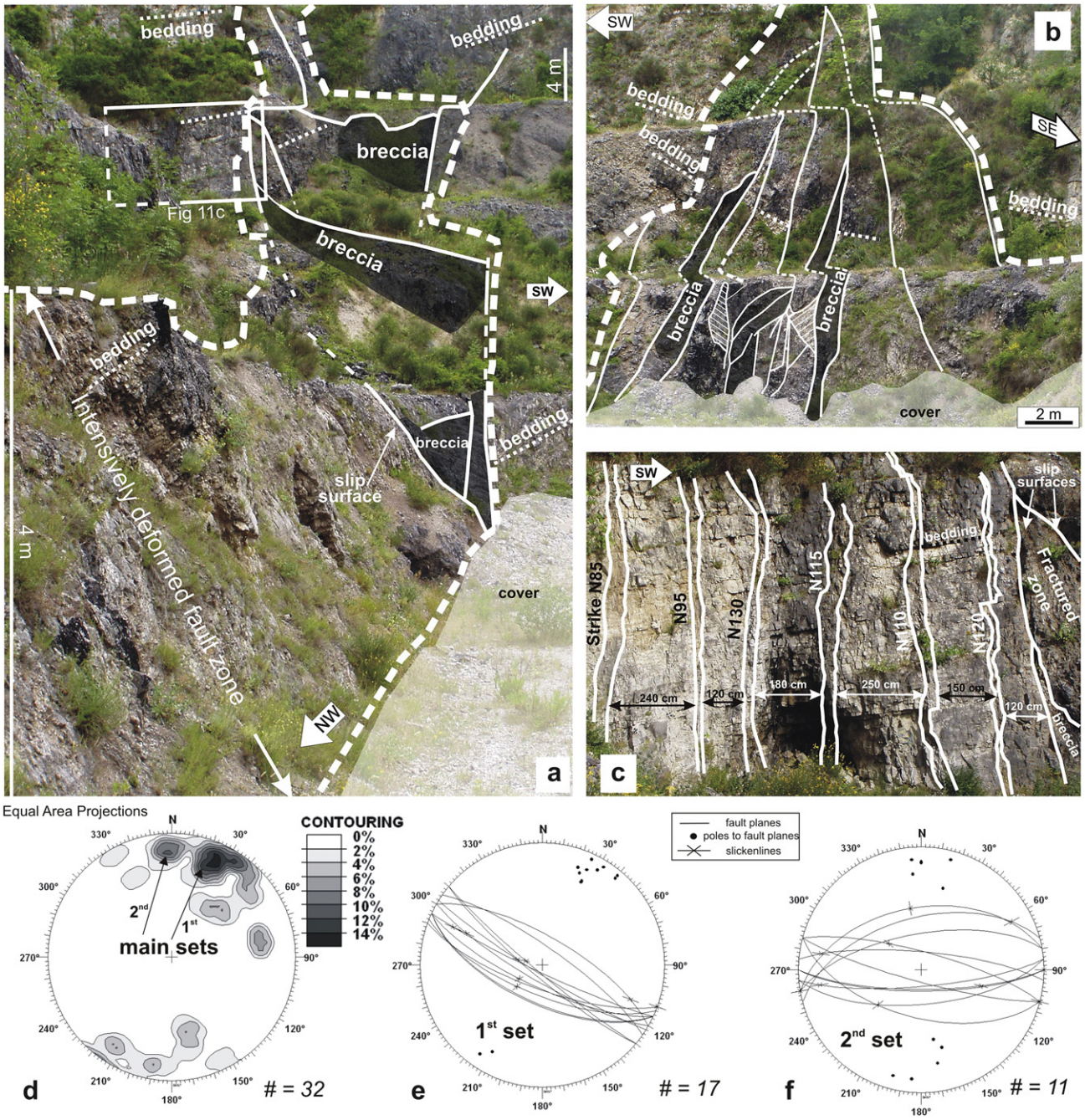

Fig. 11. (a) Cross-sectional view of the NE fault zone due to north. The fault zone contains an inner intensively deformed zone flanked by less-deformed carbonates. The former is made up of slip surfaces, fault breccias, and highly fragmented carbonates. The white rectangle represents the location of Fig. 11(b). (b) Cross-sectional view (due south) of the NE fault zone. (c) Cross-sectional view of the fracture clusters present within the hanging of all damage zone of the NE fault. (d) Lower hemisphere equal area projections of the poles relative to the slip surfaces measured along the NE fault. Two main sets are documented; the first one is NW–SE oriented (11e), whereas the second set is about E–W (11e). Slickenlines orientations show that the NW-oriented surfaces are mainly characterized by dip-slip components, whereas the E-oriented surfaces by strike-slip components.

4. Tar distribution

Tar distribution within the Roman Valley Quarry is used as a marker to characterize the fracture and fault control on hydrocarbon migration and accumulation (Fig. 12(a)). Based on the distribution of tar, we identify three main tar-rich domains: (i) fault breccia, (ii) fractured and fragmented carbonates, and (iii) undeformed carbonate rocks.

(i) The fault breccia is composed of coarse and angular grains crosscut by PS, sheared PS, isolated and discontinuous slip surfaces, and it is bounded by major slip surfaces (Fig. 12(b) and (c)). These rocks are laterally continuous along the SW fault but occur in isolated triangular bodies along the NE fault, are always impregnated by tar. The pervasiveness of tar infilling suggests that the fault breccias are excellent repositories for hydrocarbons.

(ii) Tar-rich fractured and fragmented carbonate rocks are mainly present in the damage zones of the SW and NE faults, as well as along smaller faults of the quarry (Fig. 12(a)). The through-going slip surfaces present in these rocks are coated by hydrocarbons that, eventually, moved through the surfaces

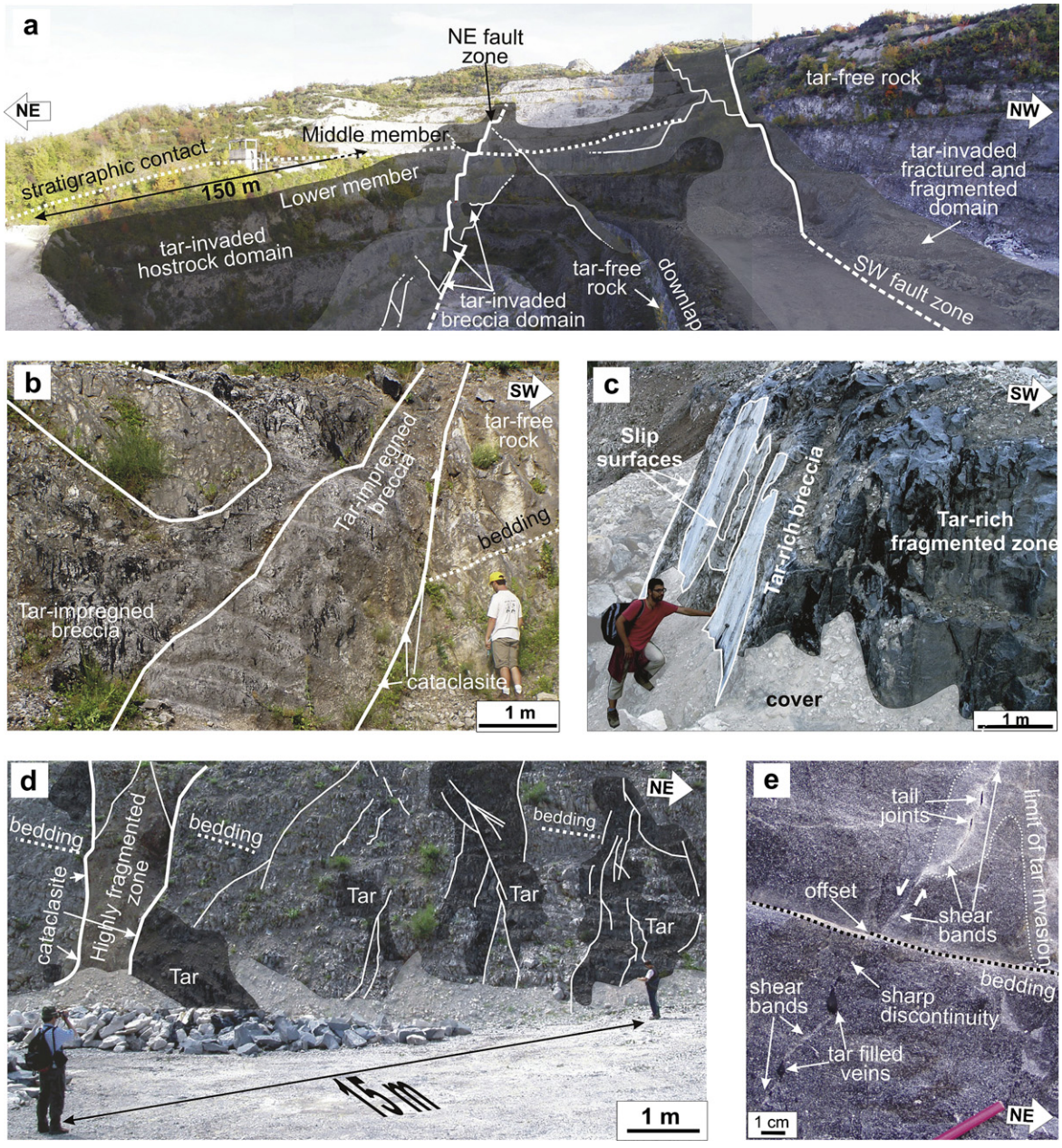

Fig. 12. (a) Tar distribution along the Roman Valley Quarry, view due north. The stratigraphic contact between lower and middle members of Bolognano Formation is shown, as well as the three main tar-invaded domains: (i) fault breccias, (ii) fractured and fragmented carbonates, (iii) undeformed host rocks. (b) Triangular-shaped, tar-invaded fault breccia present along the NE fault. (c) Cross-sectional view of the SW fault core, showing tar invasion in both fault breccia and fragmented carbonates but not in the cataclasites. Tar-invaded formation zone, made up of unfaulted carbonate grainstone flanking the SW fault zone on the hanging wall side. The influence of pre-existing shear bands on hydrocarbon migration is highlighted. The yellow dotted rectangle reports the location of Fig. 6(b). (d) Tar-invaded fractured and fragmented rock domain present in the hanging wall damage zone of the SW fault zone. (e) Through-going slip surface connecting several pre-existing shear bands, which are linked by opening-mode fractures. The normal offset along this surface is about 0.5 cm. The limit of tar invasion in the porous carbonates is reported by the white dotted line. (For interpretation of the references to colour in this figure legend, the reader is referred to the web version of this article).

spreading into the fractures and sheared fractures they intersected (Fig. 12(d) and (e)). Based on the orientation of these slip surfaces (cf. Fig. 11(d–f)), the fault parallel hydrocarbon flow in the fault damage zones was more prominent relative to cross-fault fluid flow.

(iii) Tar-rich undeformed carbonate host rocks flank the SW and NE faults (Fig. 12), consistent with high values of primary φ of these rocks. In the most porous carbonate beds (φ up to 30%), bed-parallel compaction bands and oblique shear bands may have inhibited the fluid flow (cf. Figs. 4(b) and 12(e)). Within the quarry, we also observe tar-free, marl-rich carbonate beds with low values of porosity (φ down to 5%) flanking the SW fault, which are impermeable units as far as hydrocarbon flow is concerned (Fig. 12(a)).

Our observations are consistent with most of the hydrocarbon flow postdating faulting and fracturing of the carbonate rocks. At a large scale, based on the structural setting of the northern Majella Mountain, the distribution of the tar (cf. Fig. 2(a)), and the aforementioned fault architectures, we infer that the major faults formed the principle pathways to subsurface fluid flow. We assess that hydrocarbons were channeled along these faults at certain depths, then migrated upward mainly within the deformed carbonates present at the extensional jogs of interacting oblique normal faults (Crider, 2001). As the location of the Roman Valley Quarry oil show suggests (cf. inset of Fig. 2(a)), these extensional jogs played a key role in the focusing of pronounced hydrocarbon flows. Subsequently, during their ascent, hydrocarbons also migrated laterally through the surrounding porous carbonate beds and along the smaller faults that intercepted the main fluid conduits.

5. Discussion

We compile the structures into three different categories based on the event in which they formed: (i) burial-related assemblage, (ii) early thrusting and folding assemblage, due to Middle–Upper Pliocene shortening, and (iii) oblique normal faulting assemblage, due to deformation that initiated with folding of the carbonate beds and continued during uplift and exhumation of the Majella Mountain.

5.1. Burial-related structural assemblage

The first assemblage of structures that formed within the carbonate grainstones was bed-parallel pressure solution seams, PS1, and bed-parallel compaction bands, CB (Fig. 13(a)). Based on the available geological information, these structural elements developed during burial diagenesis at overburden pressures <15 MPa (<1 km, Vezzani and Ghisetti, 1998). The bed-parallel PS1 formed both within the individual carbonate beds and at the marl-rich bed contacts, as already documented in the Majella Mountain for both platform (Graham et al., 2003) and basinal carbonate rocks (Antonellini et al., in press). The compaction bands, which do not show any evidence of shearing, can be considered as end members of volumetric deformation bands (Aydin et al., 2006). These features formed in the most porous carbonate beds (φ up to ~30%, Rustichelli personal communication). Our estimates of host rock porosity and overburden pressures are consistent with those reported, after experimental results of limestone samples deformed by pore collapse and compaction localization, by Vajdova et al. (2004). The lower porosity values of the compaction bands appear to enhance the formation and localization of PS1 within the compaction bands (cf. inset of Fig. 4(a)). This is consistent with changing deformation mechanisms of the porous carbonate grainstones through time, similar to what Tondi et al. (2006) have reported from nearby outcrops of the Orfento Formation.

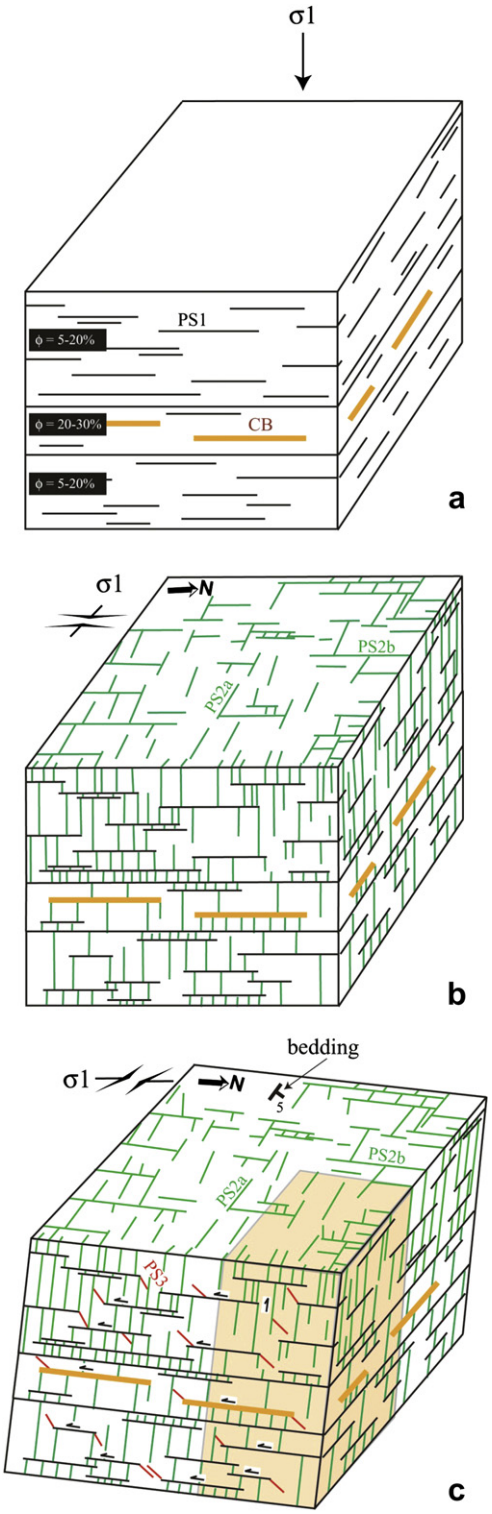

Fig. 13. Conceptual model of (a) sedimentary burial-related, (b) pre-tilting thrusting, and (c) syn-tilting thrusting structural assemblages. See text for explanation.

5.2. Early thrusting and folding structural assemblage

The early thrusting and folding assemblage includes two orthogonal sets of bed-perpendicular pressure solution seams,

PS2a and PS2b, which we infer developed when the beds were still flat (pre-tilting, Fig. 13(b)), and one set of oblique pressure solution seams, PS3, which we assess formed during folding of the carbonate beds (syn-tilting, Fig. 13(c)). Both PS2a and PS2b abut against PS1, and show mutual abutting relations. For this reason, we consider these two orthogonal PS more or less contemporaneous. In order to explain their coeval development, given that pressure solution seams represent closing-mode failure occurring perpendicular to the greatest principle stress axis (Fletcher and Pollard, 1981), we invoke a systematic reversal in the greatest and least principle stress axes. This mechanism of stress relaxation is similar to what Bai et al. (2002) modeled for orthogonal cross joints, and analogous to what Agosta and Aydin (2006) and Antonellini et al. (in press) already proposed for orthogonal pressure solution seams. The systematic changes in relative magnitudes of the principle stress axes may have been induced by relative relaxation of the σ_{hmax} axis. In this case, the ~E–W oriented σ_{hmax} and ~N–S oriented σ_{hmin} axes, associated with shortening of the central Apennines (Bigi et al., 1992; Vezzani and Ghisetti, 1998) and responsible to the formation of PS2a, locally switched due to relaxation and reloading producing the orthogonal PS2b.

The oblique PS3 terminate against the sheared bed-parallel and bed-perpendicular pressure solution seams (cf. Fig. 3(a)). In order to explain their formation, we use the relation between a sheared fracture and its tail pressure solution seams at the contractional quadrants, as documented by Rispoli (1981); Willemse et al. (1997); Graham et al. (2003); Agosta and Aydin (2006) Antonellini et al. (in press), and modeled by Fletcher and Pollard (1981), and Petit and Mattauer (1995). The occurrence of PS3 marked a new stage of deformation in carbonate rocks, which took place during ongoing-thrusting of the Majella Unit over outer thrust sheets (Vezzani and Ghisetti, 1998). The progressive rotation of the carbonate beds during folding by flexural slip (Twiss and Moores, 1992, and references therein), caused reverse shearing, top-to-the-south directed, of the pre-existing bed-parallel and bed-perpendicular elements. PS3 oriented ~E–W and dipping 45°–70° N (cf. Fig. 5(d)) were then produced at the contractional quadrants and irregularities of reversely sheared PS1, primarily, and reversely sheared PS2a and PS2b. Our conclusion suggests a sub-horizontal σ_{hmax} axis oriented ~N–S, which is about orthogonal to the regional E–W oriented σ_{hmax} axis. We infer that this 90° switch of the σ_{hmax} axis occurred in response to the build-up of the northern edge of the Majella anticline, which leads to the northward tilting of the carbonate beds that now strike at a high-angle to the fold axes (cf. Figs. 1(a) and 2(a)). This type of deformation can be associated with concurrent thrusting and folding of a layered media over lateral ramps, as sketched by Ramsay and Huber (1987).

5.3. Oblique normal faulting assemblage

The observed faults have been classified into four different classes according to their total lengths and offsets. Based on the relative timing of the specific structural elements associated to the individual fault classes, and previous knowledge on carbonate deformation (cf. Section 1), we propose a three-stages conceptual model of fault nucleation and development. The three stages are named initial, intermediate and mature, respectively.

5.3.1. Initial stage

We propose that faulting initiated by both normal and left-lateral shearing of the pre-existing, primarily bed-perpendicular, structural elements (Fig. 14(a)). This caused the formation of small, bed-bounded, isolated slip surfaces, which eventually evolved due to newly formed tail pressure solution seams at their contractional quadrants. PS4 formed primarily along normal sheared PS2a and PS2b, consistent with incipient normal faults oriented either ~WNW with southern dip or ~NNE with western dip. PS5 developed, more or less, at the same time due to left-lateral shearing of PS2a. Even though we documented on a few outcrops that PS5 postdate PS4, in this conceptual model we consider them coeval. This deformation occurred under a loading condition consistent with an E–W oriented σ_{hmax} axis with a magnitude similar to the one that acted along the vertical direction, σ_v.

Shear banding occurred only in the most porous carbonate beds, forming tabular bands showing porosity reduction and predominant normal components of slip. For this reason, these features are classified as compactive shear bands (Aydin et al., 2006), which occurred as single bands or as zones of several individual bands. As already documented for similar features crosscutting the Orfento Formation (Tondi et al., 2006), shear banding was characterized by particulate flow that involved grain translation and rotation with pore collapse. This mechanism was reported after experimental studies under low-to-high mean stresses, which ranged from 11 to 450 MPa, for limestone samples with porosity values up to 45% (Baud et al., 2000; Vajdova et al., 2004).

5.3.2. Intermediate stage

The intermediate stage of faulting was characterized by pronounced opening-mode failure, as well as dilation of the favourably oriented, pre-existing structural features (Fig. 14(b)). This switch of the fundamental failure modes, from predominant closing-mode fracturing (a time-dependent, slow process) to opening-mode fracturing (a dynamic or quasi-dynamic, brittle process) may have taken place during ongoing exhumation of the whole Majella Mountain (Ghisetti and Vezzani, 2002).

Tail joints and veins formed at the extensional quadrants of sheared pressure solution seams, contributing to the development of through-going slip surfaces. Coalescence of these sub-vertical joints and veins with the pre-existing PS, either perpendicular or oblique to bedding, defined small pods of fragmented rocks within the individual carbonate beds. With ongoing deformation the fragmented pods originally pertaining to different beds were juxtaposed, forming thicker zones of fragmented carbonates. This mechanism is widely documented for faults that developed by predominant opening-mode failure (see Segall and Pollard, 1983; Martel, 1990, for granites, Davatzes and Aydin, 2003; Myers and Aydin, 2004; Flodin and Aydin, 2004, for sandstones, Dholakia et al., 1998, for siliceous shales, Graham et al., 2003; Agosta and Aydin, 2006; Antonellini et al., in press, for carbonate rocks).

During this stage, minor pressure solution also took place at the contractional quadrants of the individual slip surfaces and at the contractional jogs of interacting slip surfaces. These two mechanisms were either active at the same time during fault creep, which implies a slow opening of joints, or during co-seismic (jointing) and inter-seismic (dissolution) deformation. Based on the available data, neither one of the two options can be discarded. During this faulting stage, we also propose that brecciation localized around the evolving main slip surfaces of the oblique faults, forming discontinuous pods of fault breccias which therefore developed proto fault cores.

5.3.3. Mature stage

In our conceptual model, a mature stage of faulting occurred along the SW and NE faults with strain localized around the major slip surfaces, which allowed them to develop to a few km in length and to accumulate up to several 10s of m offsets. Strain localization caused the intense brecciation and fragmentation, as well as cataclastic deformation, of the fault cores (Fig. 14(c)). Brecciation occurred primarily at the jogs formed by interacting fault segments, and in correspondence of slip surface intersections. Cataclasis

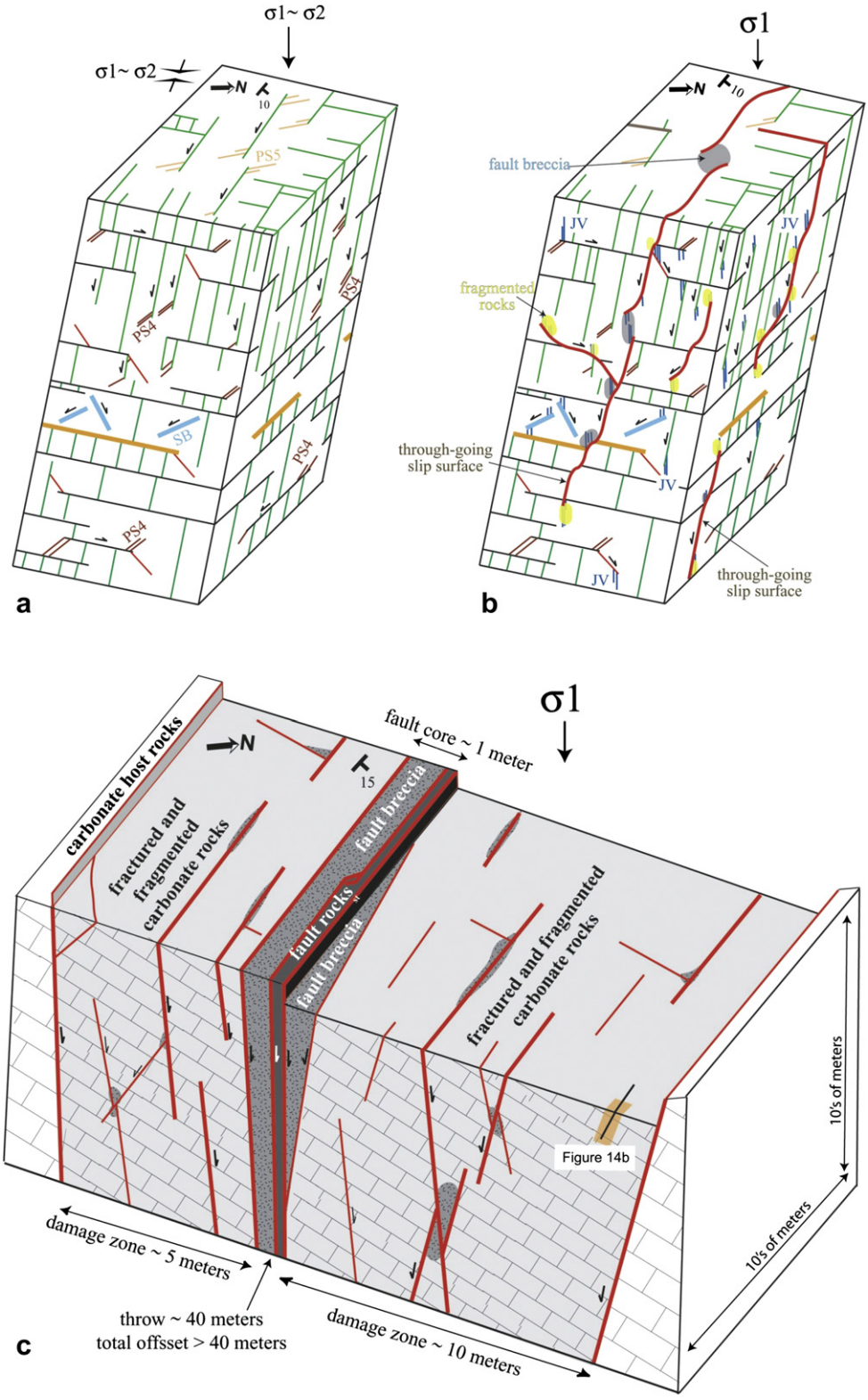

Fig. 14. Conceptual model of oblique normal faulting, (a) incipient faulting stage, (b) intermediate faulting stage, (c) mature faulting stage. See text for explanation.

mainly took place along the major slip surfaces involving comminution and micro-fracturing of the carbonate grainstones. The products of this deformation, either grain-supported or matrix-supported cataclastic rocks, formed a tight rock of a few cm-thick that was eventually cemented by calcite precipitated by fault fluids. These well-developed fault cores, as thick as 1 m, were flanked by thicker damage zones affected by opening-mode failure, dilation of favourably oriented pre-existing elements, and minor faulting. Deformation of the carbonate damage zones was more pronounced at the fault hanging wall, as the asymmetric damage zone distribution would suggest (cf. Berg and Skar, 2005, and references therein).

5.4. Fault and fracture permeability

The SW fault forms a combined barrier-conduit permeability structure to fluid flow. There, the thin cataclastic rocks of the fault core, if laterally continuous along the whole fault, act as seals for cross-fault fluid flow (Micarelli et al., 2006; Agosta et al., 2007), whereas the major slip surfaces, fault breccia and the fault damage zones behave as fluid conduits (cf. Fig. 12(c)). Conversely, due to the discontinuous presence of cataclastic fault rocks and fault breccias, the NE fault forms a distributed conduit to fluid flow (cf. Fig. 12(f)). The main fluid pathways are provided by the numerous slip surfaces, which enhance the fault parallel fluid flow, whereas the main fluid repositories are represented by the thick lithon- and triangular-shaped fault breccias.

Small and medium faults, which may include isolated and/or through-going slip surfaces, fractures, sheared fractures, and isolated pods of fault breccia, form single conduit permeability structures to fluid flow. Based on our observations, these faults are able to focus on hydrocarbons only when they intersect other hydrocarbon-bearing faults. So, despite their potential conductive behavior to fluid flow, the hydraulic connectivity of these faults to larger fluid conduits is the key in channeling fluids. This is clearly shown within the Roman Valley Quarry, where isolated small and medium faults do not contain hydrocarbons. With regards to the fundamental structures, both sheared PS2a and JV are the most impregnated by tar. These two structures show the greatest aperture among all the surveyed ones of the Roman Valley Quarry (Alessandroni, 2008), suggesting that their hydraulic behavior was probably affected by the current NW-oriented σ_{hmax} of central Italy (Cello et al., 1997; Montone et al., 2004).

6. Conclusions

In this study we documented the deformation mechanisms that occurred during initiation and development of oblique normal faults in carbonate grainstones of the Bolognano Fm., Majella Mountain, central Italy. After geological mapping of the northern side of this mountain and detailed structural analysis of the faulted outcrops of the Roman Valley Quarry, we compiled the structures occurring in pristine carbonate host rocks ($5\% < \phi < 30\%$) into two different structural assemblages, burial-related and thrusting and folding, respectively. These structures constituted the background deformation of the rocks later involved in oblique normal faulting.

Oblique normal faulting initiated with folding by flexural slip and tilting of the carbonate beds, and continued during ongoing uplift and exhumation of the whole Majella Mountain. Based on the documented fundamental failure modes and mechanisms of fault development, we proposed a conceptual model comprised of three main stages of faulting. The initial stage was characterized by the nucleation of oblique normal faults due to shearing of the pre-existing structures, which produced tail pressure solution seams at the contractional quadrants of the sheared parent fractures. In the most porous carbonate beds (ϕ up to 30%), compactive shear bands formed by particulate flow that involved grain translation and rotation with pore collapse.

Oblique normal faults evolved due to the linkage of the bed-bounded, discontinuous slip surfaces across contiguous carbonate beds, which produced mainly tail opening-mode fractures at their extensional quadrants and within releasing jogs. This deformation mechanism enhanced the degree of carbonate deformation, and formed isolated pods of fragmented rocks along the through-going slip surfaces. Brecciation also took place along these surfaces and at their intersections. The mature stage of faulting was mainly characterized by strain localization around the major slip surfaces of the faults, with brecciation and cataclastic deformation of the fault cores. These deformation mechanisms formed grain- and matrix-supported cataclastic rocks and fault breccias. Conversely, the carbonate damage zones surrounding the fault cores were affected by predominant opening-mode failure and dilation of the favourably oriented pre-existing structures, as well as development of small and medium faults.

Presence of hydrocarbons in the form of tar along some of the study outcrops of the quarry was used as a proxy to assess the fracture and fault control on fluid flow. Most of the hydrocarbon flow postdated fracturing and faulting of the carbonates, and took place in three main domains: (i) fault breccia, (ii) fractured and fragmented carbonates, and (iii) undeformed porous carbonate grainstones. The thin cataclastic rocks present along the SW and NE faults did not show any presence of tar neither in the matrix nor in the survivor clasts. For this reason, if continuous along the fault cores, these rocks therefore formed seals for cross-fault fluid flow (cf. Micarelli et al., 2006; Agosta et al., 2007; Agosta et al., 2008). On the contrary, both fault breccias and fault damage zones formed conduits for fluid flow. Based on the orientation of the major slip surfaces and small and medium faults they contain, the fault parallel fluid flow was dominant in the carbonate damage zones. Considering their internal architecture, these small and medium faults acted individually as single conduits to fluid flow. At a larger scale, we observe that hydrocarbons focussed within extensional fault jogs, as the location of the Roman Valley Quarry suggests.

Acknowledgements

We thank Andrea Rustichelli and Paolo Vallesi for their help during field work, and both Marco Antonellini and Matthias Braun for useful discussions on the hydraulic properties of the deformed carbonate rocks. We also thank the careful revision and useful suggestions provided by the editor, T. Blenkinsop, and the referees F. Storti and S. Mazzoli. This work was financed by the Faults and Fractures in Carbonates project of the University of Camerino, and the Rock Fracture Project of Stanford University.

References

Agosta, F., Kirschner, D.L., 2003. Fluid conduits in carbonate-hosted seismogenic normal faults of Central Italy. Journal of Geophysical Research 108 (B4), 2221. doi:10.1029/2002JB002013.

Agosta, F., Aydin, A., 2006. Architecture and deformation mechanism of a basin-bounding normal fault in Mesozoic platform carbonates, central Italy. Journal of Structural Geology 28, 1445–1467.

Agosta, F., Prasad, M., Aydin, A., 2007. Physical properties of carbonate fault rocks, Fucino Basin (Central Italy): implications for fault seal in platform carbonates. Geofluids 7, 19–32.

Agosta, F., Mulch, A., Chamberlain, P., Aydin, A., 2008. Geochemical traces of CO_2-rich fluid flow along normal faults of central Italy. Geophysical Journal International 174, 758–770.

Alessandroni, M., 2008. Structural Control on the Flow and Accumulation of Hydrocarbons in Carbonate Grainstones: an Example from the Bolognano Fm. (Majella Mt. Italy). Ph.D. thesis, University of Camerino, 167 pp.

Alvarez, W., Engelder, T., Geiser, P.A., 1978. Classification of solution cleavage in pelagic platform carbonates. Geology 6, 263–266.

Antonellini, M., Aydin, A., 1994. Effect of faulting on fluid flow in porous sandstones: petrophysical properties. American Association of the Petroleum Geologists Bulletin 78, 355–377.

Antonellini, A., Tondi, E., Aydin, A., Agosta, F., Failure modes in basin carbonates and their impact on fault development, Majella Mountain, central Italy. Marine and Petroleum Geology, doi:10.1016/j.marpetgeo.2007.10.008. in press.

Aydin, A., 2000. Fractures, faults, and hydrocarbon entrapment, migration and flow. Marine and Petroleum Geology 17, 797–814.

Aydin, A., Borja, I.R., Eichhubl, P., 2006. Geological and mathematical framework for failure modes in granular rocks. Journal of Structural Geology 28, 83–98.

Aydin, A., Antonellini, M., Tondi, E., Agosta, F. Deformation along the leading edge of the Majella thrust sheet, Fara San Martino, central Italy. Journal of Structural Geology, (this issue).

Bai, T., Maerten, L., Gross, M.R., Aydin, A., 2002. Orthogonal cross joints: do they imply a regional stress rotation? Journal of Structural Geology 24, 77–88.
Bally, A.W., Burbi, L., Cooper, C., Ghelardoni, R., 1988. Balanced sections and seismic reflection profiles across the central Apennines. Memorie della Società Geologica Italiana 35, 257–310.
Baud, P., Schubnel, A., Wong, T.F., 2000. Dilatancy, compaction, and failure mode in Solnhofen limestone. Journal of Geophysical Research 105 (B8), 19289–19303.
Berg, S.S., Skar, T., 2005. Controls on damage zone asymmetry of a normal fault zone: outcrop analysis of a segment of the Moab fault, SE Utah. Journal of Structural Geology 27, 1803–1822.
Bigi, G., Cosentino, D., Parotto, M., Sartori, R., Scandone, P., 1992. Structural model of Italy, scale 1:500,000, 6 sheets. CNR, Quaderni di Ricerca Scientifica 114.
Billi, A., Salvini, F., Storti, F., 2003. The damage zone-fault core transition in carbonate rocks: implications for fault growth, structure and permeability. Journal of Structural Geology 25, 1779–1794.
Billi, A., 2005. Grain size distribution and thickness of breccia and gouge zones from thin (<1 m) strike-slip fault cores in limestones. Journal of Structural Geology 27, 1823–1837.
Blenkinsop, T.G., 1991. Cataclasis and processes of particle size reduction. Pure and Applied Geophysics 136, 59–86.
Caine, J.S., Evans, J.P., Forster, C.B., 1996. Fault zone architecture and permeability structure. Geology 24, 1025–1028.
Casnedi, R., 1983. Hydrocarbon-bearing submarine fan system of Cellino Formation, Central Italy. Memorie della Società Geologica Italiana 67, 359–370.
Cello, G., Mazzoli, S., Tondi, E., Turco, E., 1997. Active tectonics in the central Apennines and possible implications for seismic hazard analysis in peninsular Italy. Tectonophysics 272, 43–68.
Chester, F.M., Logan, J.M., 1986. Composite planar fabric of gouge from the Punchbowl fault, California. Journal of Structural Geology 9, 621–634.
Chester, F.N., Evans, J.P., Biegel, R.L., 1993. Internal structure and weakening mechanisms of the San Andreas fault. Journal of Geophysical Research 98, 771–786.
Cowie, P.A., Scholz, C.H., 1992. Growth of faults by accumulation of seismic slip. Journal of Geophysical Research 97, 11085–11095.
Crescenti, U., Crostella, A., Donzelli, G., Raffi, G., 1969. Stratigrafia della serie calcarea dal Lias al Miocene nella regione marchigiano-abruzzese. Memorie della Società Geologica Italiana 8, 343–420.
Crider, J., 2001. Oblique slip and the geometry of normal fault linkage: mechanics and a case study from the basin and range in Oregon. Journal of Structural Geology 12, 1997–2009.
Davatzes, N.C., Aydin, A., 2003. The formation of conjugate normal fault systems in folded sandstone by sequential jointing and shearing, Waterpocket Monocline, Utah. Journal of Geophysical Research 108 (B10), 2478. doi:10.1029/2002JB002289.
Dholakia, S.K., Aydin, A., Pollard, D.D., Zoback, M.D., 1998. Fault-controlled hydrocarbon pathways in the Monterey Formation, California. American Petroleum Geologists Bulletin 82, 1551–1574.
Donzelli, G., 1997. Studio geologico della Maiella. Memorie della Società Geologica Italiana 67, 359–370.
Eberli, G., Bernoulli, D., Sanders, D., Vecsei, A., 1993. From aggradation to progradation: the Maiella platform, Abruzzi, Italy. In: Simo (Ed.), Cretaceous Carbonate Platforms. American Association of the Petroleum Geologists Memoir, vol. 56, pp. 213–232.
Fletcher, R., Pollard, D., 1981. Anticrack model for pressure solution seams. Geology 9, 419–424.
Flodin, E.A., Aydin, A., 2004. Evolution of a strike-slip fault network, Valley of Fire, southern Nevada. Geological Society of America Bulletin 116, 42–59.
Flodin, E.A., Gerdes, M., Aydin, A., Wiggins, W.D., 2005. Petrophysical properties of cataclastic fault rock in sandstone. In: Sorkhabi, R., Tsuji, Y. (Eds.), Faults and Petroleum Traps. American Association of the Petroleum Geologists Memoir, vol. 85, pp. 197–217.
Ghisetti, F., Vezzani, L., 1998. Geometrie deformative ed evoluzione cinematica dell'Appennino centrale. Studi Geologici Camerti 14, 127–154.
Ghisetti, F., Vezzani, L., 1999. Depth and modes of Pliocene–Pleistocene crustal extension of the Apennines (Italy). Terra Nova 11, 67–72.
Ghisetti, F., Kirschner, D.L., Vezzani, L., Agosta, F., 2001. Stable isotope evidence for contrasting paleofluid circulation in thrust and seismogenic normal faults of central Apennines, Italy. Journal of Geophysical Research 106, 8811–8825.
Ghisetti, F., Vezzani, L., 2002. Normal faulting, extension and uplift in the outer thrust belt of the central Apennines (Italy): role of the Caramanico fault. Basin Research 14, 225–236.
Graham, B., Antonellini, M., Aydin, A., 2003. Formation and growth of normal faults in carbonates within a compressive environment. Geology 31, 11–14.
Graham-Wall, B., Girgacea, R., Mesonjesi, A., Aydin, A., 2006. Evolution of fluid pathways through fracture controlled faults in carbonates of the Albanides fold-thrust belt. American Association of Petroleum Geologists Bulletin 90, 1227–1249.
Kelly, P.G., Peacock, D.C.P., Sanderson, D.J., 1998. Linkage and evolution of conjugate strike-slip fault zones in platform carbonates of Somerset and Northumbria. Journal of Structural Geology 20, 1477–1493.
Kim, Y.S., Peacock, D.C.P., Sanderson, D.J., 2003. Mesoscale strike-slip faults and damage zones at Marsalforn, Gozo Island, Malta. Journal of Structural Geology 25, 793–812.
Kim, Y.S., Peacock, D.C.P., Sanderson, D.J., 2004. Fault damage zones. Journal of Structural Geology 26, 503–517.
Lampert, S.A., Lowrie, W., Hirt, A.M., Bernoulli, D., Mutti, M., 1997. Magnetic and sequence stratigraphy of redeposited Upper Cretaceous limestones in the Montagna della Majella, Abruzzi, Italy. Earth and Planetary Science Letters 150, 79–83.
Marchegiani, L., Van Dijk, J.P., Gillespie, P.A., Tondi, E., Cello, G., 2006. Special Publications. Scaling properties of the dimensional and spatial characteristics of fault and fracture systems in the Majella Mountain, central Italy, vol. 261. Geological Society of London, pp. 113–131.
Marshak, S., Geiser, P.A., Alvarez, W., Engelder, T., 1982. Mesoscopic fault array of the northern Umbrian Apennine fold belt: geometry of conjugate shear by pressure-solution slip. Geological Society of America Bulletin 93, 1013–1022.
Martel, S.J., 1990. Formation of compound strike-slip fault zones, Mount Abbot quadrangle, California. Journal of Structural Geology 12, 869–882.
Mazzoli, S., Di Bucci, D., 2003. Critical displacement for normal fault nucleation from en-echelon vein arrays in limestones: a case study from the southern Apennines (Italy). Journal of Structural Geology 25, 1011–1020.
Micarelli, L., Benedicto, A., Wibberley, C.A.J., 2006. Structural evolution and permeability of normal fault zones in highly porous carbonate rocks. Journal of Structural Geology 28, 1214–1227.
Mollema, P.N., Antonellini, M., 1999. Development of strike-slip faults in the dolomites of the Sella Group, northern Italy. Journal of Structural Geology 21, 273–292.
Montone, P., Mariucci, M.T., Pondrelli, S., Amato, S., 2004. An improved stress map for Italy and surrounding regions (central Mediterranean). Journal of Geophysical Research 109 B10410.
Mort, K., Woodcock, N.H., 2008. Quantifying fault breccia geometry: Dent Fault, NW England. Journal of Structural Geology 30, 701–709.
Myers, R., Aydin, A., 2004. The evolution of faults formed by shearing across joint zones in sandstones. Journal of Structural Geology 26, 947–966.
Odling, N.E., Harris, S.D., Knipe, R.J., 2004. Permeability scaling properties of fault damage zones in clastic rocks. Journal of Structural Geology 26, 1727–1747.
Patacca, E., Scandone, P., Bellatalla, M., Perilli, N., Santini, U., 1992. La zona di giunzione tra l'arco appenninico settentrionale e l'arco appenninico meridionale nell'Abruzzo e nel Molise. In: Tozzi (Ed.), Studi preliminari all'acquisizione dati del profilo CROP 11 Civitavecchia-Vasto. Studi Geologici Camerti, pp. 417–441.
Petit, J.P., Mattauer, M., 1995. Paleostress superimposition deduced from mesoscale structures in limestone: the Matelles exposures. Languedoc, France. Journal of Structural Geology 17, 245–256.
Pollard, D., Aydin, A., 1988. Progress in understanding jointing over the past century. Geological Society of America Bulletin 100, 1181–1204.
Rawling, G.C., Goodwin, L.B., Wilson, J.L., 2001. Internal architecture, permeability structure, and hydrologic significance of contrasting fault-zone types. Geology 29, 43–46.
Ramsay, J.G., Huber, M.I., 1987. Modern Structural Geology, vol. II. Academic Press, pp. 309–462.
Rispoli, R., 1981. Stress fields about strike-slip faults inferred from stylolites and tension gashes. Tectonophysics 75, 29–36.
Salvini, F., Billi, A., Wise, D.U., 1999. Strike-slip fault-propagation cleavage in carbonate rocks: the Mattinata fault zone, Southern Apennines, Italy. Journal of Structural Geology 21, 1731–1749.
Scisciani, V., Tavarnelli, E., Calamita, F., 2002. The interaction of extensional and contractional deformation in the outer zones of the Central Apennines, Italy. Journal of Structural Geology 24, 1647–1658.
Segall, P., Pollard, D.D., 1983. Nucleation and growth of strike slip faults in granite. Journal of Geophysical Research 88, 555–568.
Selli, R., 1960. Il Messiniano Mayer-Eymar 1867. Proposta di un neostratotipo. In: Giornale di Geologia, vol. 28, Bologna.
Sibson, R.H., 1977. Fault rocks and fault mechanisms. Journal of the Geological Society of London 133, 191–213.
Storti, F., Billi, A., Salvini, F., 2003. Particle size distributions in natural carbonates fault rocks: insights for non-self-similar cataclasis. Earth and Planetary Science Letters 206, 173–186.
Tondi, E., Antonellini, M., Aydin, A., Marchegiani, L., Cello, P., 2006. The roles of deformation bands and pressure solution seams in fault development in carbonate grainstones of the Majella Mountain, Italy. Journal of Structural Geology 28, 376–391.
Tondi, E., 2007. Nucleation, development and petrophysical properties of faults in carbonate grainstones: evidence from the San Vito Lo Capo peninsula (Sicily, Italy). Journal of Structural Geology 29, 614–628.
Twiss, R., Moores, E.M., 1992. Structural Geology. Freeman and Company, 532 pp.
Vajdova, V., Baud, P., Wong, T., 2004. Compaction, dilatancy, and failure in porous carbonate rocks. Journal of Geophysical Research 109 B05204.
Vecsei, A., 1991. Aggradation un Progradation eines karbonatplatform-Randes: Kreide bis Mittleres Tertiär der Montagna della Maiella, Abruzzen. In: Mitteilungen aus dem Geologischen Institut der Eidgenössischen Technischen Hochschule und der Universitat Zürich, Neue Folge, vol. 294, pp. 169.
Vecsei, A., Sanders, D., Bernoulli, D., Eberli, G., Pignatti, J.S., 1998. Cretaceous to Miocene sequence stratigraphy and evolution of the Maiella carbonate platform margin, Italy. In: Hnbol (Ed.), Mesozoic and Cenozoic Sequence Stratigraphy of European Basins. Society of Sedimentary Geology Special Publication, vol. 60, pp. 53–74.
Vezzani, L., Ghisetti, F., 1998. Carta geologica dell'Abruzzo. S.EL.CA., Firenze.
Willemse, E.J., Peacock, D.C.P., Aydin, A., 1997. Nucleation and growth of strike-slip faults in platform carbonates from Somerset, U.K. Journal of Structural Geology 19, 1461–1477.